ACS APPLIED MATERIALS & INTERFACES

Research Article

www.acsami.org

Improved Performance in Diketopyrrolopyrrole-Based Transistors with Bilayer Gate Dielectrics

Tae-Jun Ha,[†] Prashant Sonar,*[,‡] and Ananth Dodabalapur*[,†]

[†]Microelectronics Research Center, The University of Texas at Austin, Austin, Texas 78758, United States

[‡]Institute of Materials Research and Engineering (IMRE), Agency for Science, Technology, and Research (A*STAR), Singapore 117602, Singapore

Supporting Information

ABSTRACT: There has been significant progress in the past 2 decades in the field of organic and polymer thin-film transistors. In this paper, we report a combination of stable materials, device architecture, and process conditions that resulted in a patterned gate, small channel length (<5 μm) device that possesses a scaled field-induced conductivity in air that is higher than any organic/polymer transistor reported thus far. The operating voltage is below 10 V; the on-off ratio is high; and the active materials are solution-processable. The semiconducting polymer is a new donor−acceptor polymer with furan-substituted diketopyrrolopyrrole and thienyl-vinylene-thienyl building blocks in the conjugated backbone. One of the major striking features of our work is that the patterned-gate device architecture is suitable for practical applications. We also propose a figure of merit to meaningfully compare polymer/organic transistor performance that takes into account mobility and operating voltage. With this figure of merit, we compare leading organic and polymer transistors that have been hitherto reported. The material and device architecture have shown very high mobility and low operating voltage for such short channel length (below 5 μm) organic/polymer transistors.

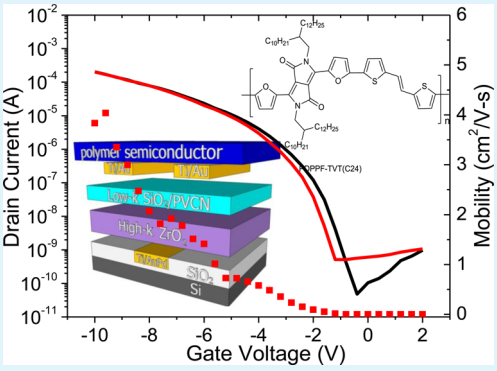

KEYWORDS: *donor−acceptor polymer, low operating voltage, small channel length, figure of merit, recessed gate, bilayer gate dielectric*

INTRODUCTION

There have been several promising reports on high-performance organic and polymer field-effect transistors in recent years.[1−5] Impressive advances have been made in improving the mobility values that routinely exceed 1 $cm^2 V^{-1} s^{-1}$.[6−15] These improvements have resulted from a combination of various parameters, such as molecular design, interface engineering (at the dielectric−semiconductor interface), device structure, and fabrication techniques. The ultimate goal of all of these studies is to come up with a practical solution where appropriate material and device geometry combinations can be implemented, which can result in very good performance and stable operation under ambient conditions. The key metrics for good performance, from a practical standpoint, include high carrier mobility, low-operating voltage, high on/off current ratio, patterned gate, air-stable operation, and small channel length. Additionally, the patterned gate will cut down coupling capacitance and facilitate higher speed operation. In addition to the above parameters, solution processability of the active materials, semiconductor and gate insulator, is a very desirable characteristic that opens up low-cost, high-throughput, and large-area fabrication processes that are important for practical applications.[16−18] Surprisingly, very few previous reports satisfy all or most of the above requirements. In this paper, we report a material combination, device geometry, and set of process conditions that meet all of the above requirements. We propose that such polymer field-effect transistor device configuration will lead to a practical device technology that can be very beneficial for display and other applications.

There are numerous requirements that have to be simultaneously satisfied to realize a high-performance practical technology for organic/polymer thin-film transistors (TFTs).[19−21] In the past 2 decades, there have been many reports of performance improvements in organic transistors of various types.[22−27] A large number of these reports are based on devices fabricated on silicon substrates with thermally grown oxide dielectrics. In single-crystal devices, air is sometimes employed at the gate dielectric.[28] In most of the reported papers, the gate is not patterned and the channel lengths are very long and defined by shadow masking of the electrode material. Promising mobility values obtained from materials in such studies are not always translatable to practical devices. In this paper, we describe the details of a technology based on a furan-substituted diketopyrrolopyrrole-based polymer material with bilayer gate dielectric combination that meets all of these requirements and results in one of the best performances for the furan-substituted diketopyrrolopyrrole (DPPF) class of materials. We have also proposed figure of merit (FOM)

Received: October 4, 2013
Accepted: February 7, 2014
Published: February 7, 2014

   dx.doi.org/10.1021/am4043646 | ACS Appl. Mater. Interfaces 2014, 6, 3170−3175

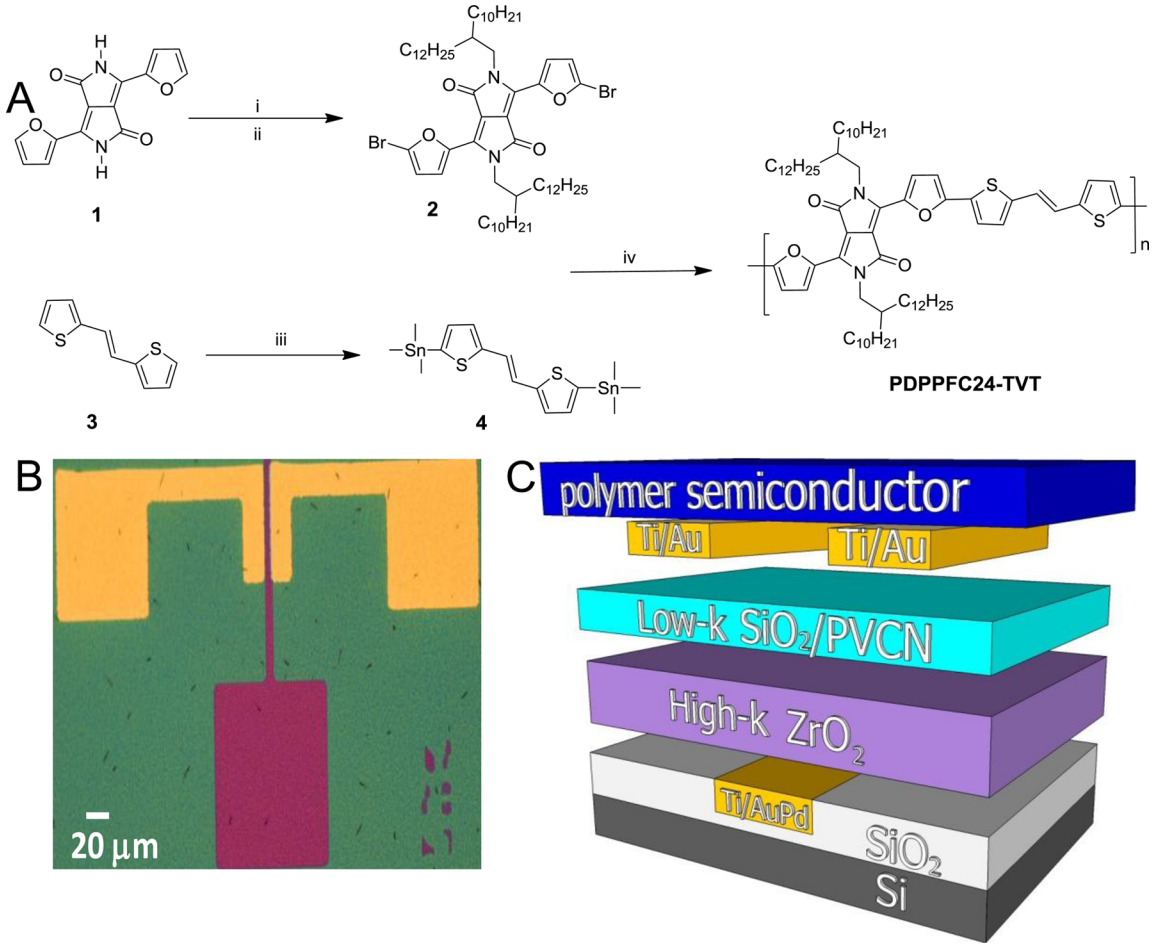

Figure 1. (A) Synthesis of PDPPFC24-TVT [reagents and conditions: (i) K_2CO_3, 2-decyl-1-tetradecyl bromide, anhydrous *N*,*N*-dimethylformamide (DMF), 120−130 °C, overnight; (ii) bromine, chloroform, room temperature, overnight; (iii) −78 °C, BuLi, tetramethylethylenediamine (TMEDA), trimethyltin chloride, tetrahydrofuran (THF)/hexane, −78 °C for 20 h; and (iv) $Pd(PPh_3)_2Cl_2$, anhydrous toluene, 90 °C for 72 h], (B) optical image of PDPPFC24-TVT TFTs possessing a channel width of 80 μm and a channel length of 4 μm, and (C) device configuration of a recessed-gate DPP-based polymer TFT employing a bilayer of high-κ and low-κ dielectrics.

characteristics to correlate and compare the various reported transistor technologies with respect to the class of materials (small molecules and polymers), device dimensions (channel length), and mobility values. The approach that we employed in this work can be advantageously used to fabricate transistors with other organic and polymer semiconductors. The FOM that we are proposing here serves as very useful to compare various TFTs, including organic, polymer, and amorphous oxide.

For practical applications, the gate must be patterned and the channel length needs to be at least in the 3−5 μm level. The operating voltage needs to be low (below 10 V), and the mobility and on/off current ratio need to be high. The typical expected mobility for various large-scale applications [display devices, logic circuits, and radio-frequency identification (RFID) tags] must be higher than 1 $cm^2\ V^{-1}\ s^{-1}$, and the on/off ratio must be $>10^6$. Additionally, the material must ideally be air-stable to ensure stable long-term operation with some passivation. Solution processability of the active organic semiconductor and the gate insulator is extremely important for large-area application using various fabrication methods, such as ink-jet printing, spray coating, and roll-to-roll printing.

EXPERIMENTAL SECTION

Figure 1 shows the chemical structure of the furan-flanked diketopyrrolopyrrole−thienylene−vinylene−thienylene (PDPPFC24-TVT) polymer and also the schematic device structure. The device design employs a recessed gate and a bilayer gate dielectric consisting of high-κ zirconium dioxide (ZrO_2) and low-κ silicon dioxide (SiO_2) or poly(vinyl cinnamate) (PVCN) dielectric. Device fabrication started with a 200 nm thick thermally grown SiO_2 on N-doped silicon substrate. The gate electrode was defined by photolithography and patterned by etching SiO_2 with a reactive ion etcher to fabricate the recessed gate. A 2.5 nm titanium (Ti) adhesion layer and a 45 nm gold−palladium (AuPd) layer as a gate electrode were deposited by thermal evaporation. A 90 nm thick ZrO_2 dielectric layer was formed by spin coating. Either thin SiO_2 or PVCN was employed as the low-κ dielectric. The capacitance value of bilayer consisting of high-κ and very thin low-κ dielectric is 230 nF/cm^2. After source/drain electrodes were defined by photolithography, Ti/Au (2.5/45 nm) layers were blanket-deposited by thermal evaporation and surface-treated with a self-assembled monolayer (SAM) of pentafluorobenzenethiol (PFBT). A 40 nm thick semiconductor film was deposited by spin coating and annealed at 200 °C for 30 min under an inert atmosphere. PDPPFC24-TVT TFTs possess a channel width of 80 μm and a channel length of 4 μm, as shown in Figure 1. All samples were characterized by a semiconductor parameter analyzer in air.

dx.doi.org/10.1021/am4043646 | ACS Appl. Mater. Interfaces 2014, 6, 3170−3175

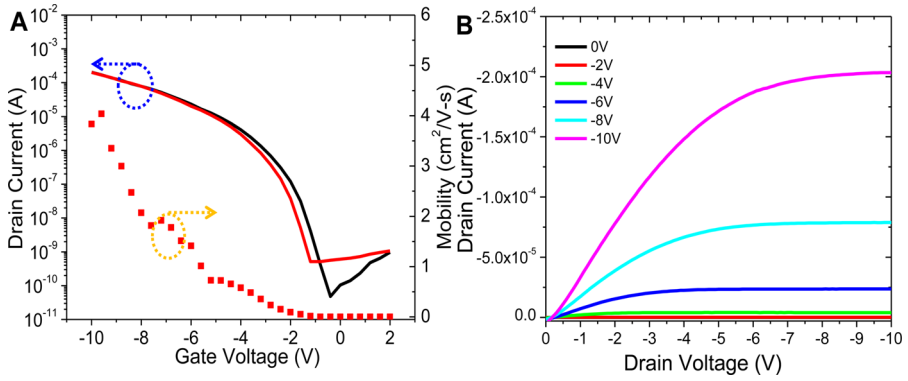

Figure 2. (A) Transfer characteristics during the sweep of gate voltage (between −10 and 2 V) in both forward and reverse directions measured in normal air and the field-effect mobility as a function of the gate voltage. Very little hysteresis is observed, and the devices exhibit a field-effect mobility of up to 4.2 $cm^2\ V^{-1}\ s^{-1}$. (B) Output characteristics of recessed-gate PDPPFC24-TVT TFTs employing bilayers of high-κ and low-κ dielectrics.

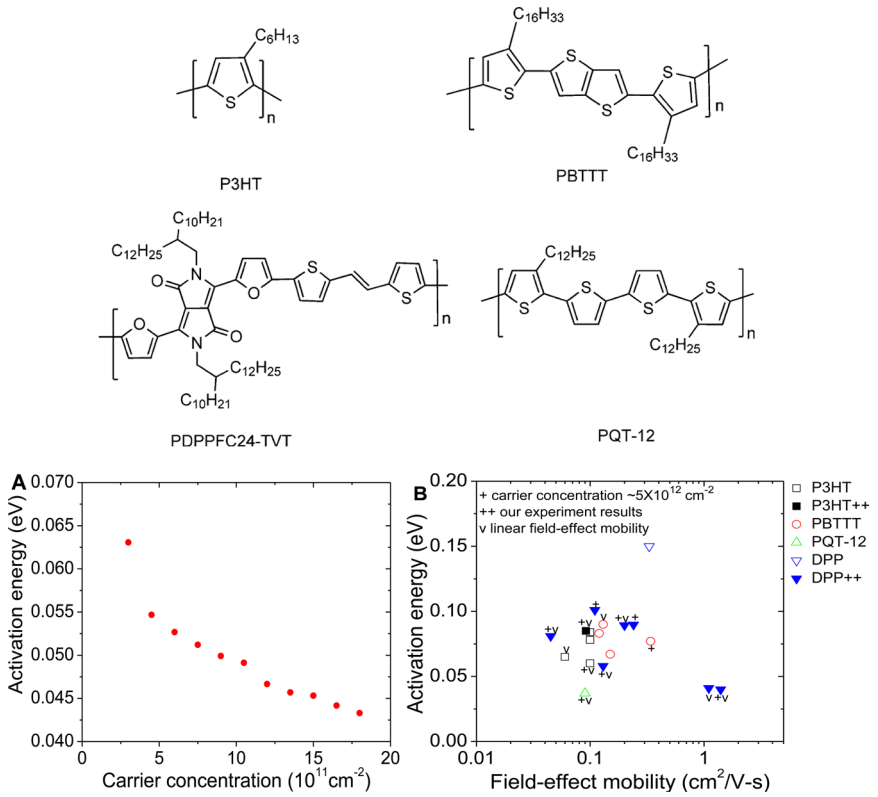

Figure 3. (A) Activation energies as a function of the channel carrier concentration in PDPPFC24-TVT TFTs. The magnitude of the lowest activation energy (~40 meV) is relatively small in comparison to measurements made with other DPP-based semiconductors and (B) activation energies as a function of field-effect mobility in various polymer semiconductor-based transistors (see the respective chemical structures above the graphs). Data are from refs 35 and 39−49.

RESULTS AND DISCUSSION

The rationale for the recessed-gate structure is to present as little surface relief before the deposition of the gate insulator. This will improve the reliability of the insulator and keep down leakage currents. The thin, low-κ insulator is employed adjacent to the polymer semiconductor to minimize polarization-induced Fröhlich polaron effects, which result when polarizable semiconductors, such as organic semiconductors, are in close proximity to polar media, such as high-κ dielectrics or polar vapors.[29,30] Additionally, the density of interface traps may be reduced, which can improve mobility further. In the absence of such low-κ interfacial layers, the field-effect mobility is significantly lower.[31] To enhance the molecular ordering, SAM surface treatments of the dielectric are performed. Such molecular ordering modifies the surface energy at the interface, which leads to better charge carrier injection and improved electrical contacts.[32,33] The PDPPFC24-TVT-based TFT devices exhibit a field-effect mobility of up to 4.2 $cm^2\ V^{-1}\ s^{-1}$, a threshold voltage (V_{th}) of −1 V, an on/off current ratio of 1×10^7, and a sub-threshold swing (S.S.) of 0.3 V/decade for low-gate-voltage operation (<10 V) when tested in normal air. The transfer and output characteristics of TFT devices are shown in Figure 2. Very little hysteresis is observed during the sweep of gate voltage in both forward and reverse directions.

dx.doi.org/10.1021/am4043646 | ACS Appl. Mater. Interfaces 2014, 6, 3170−3175

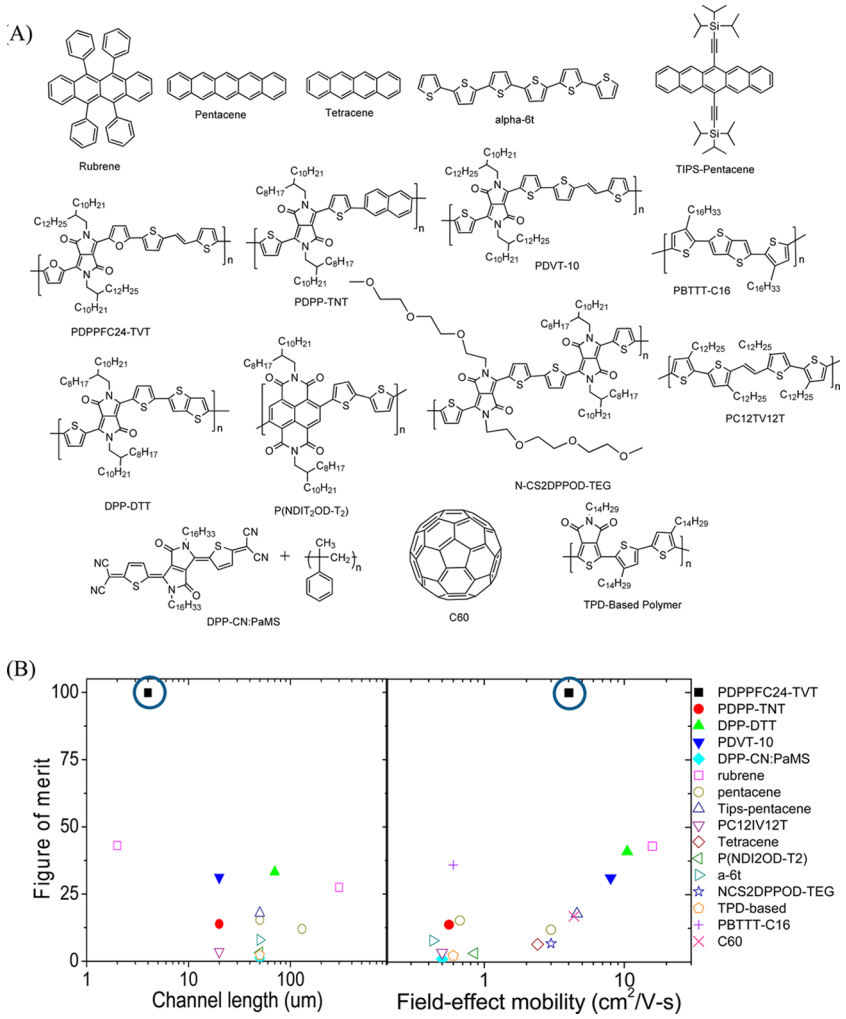

Figure 4. (A) Chemical structures of the compounds used for the FOM study and (B) FOM as functions of channel length and field-effect mobility on various organics and polymers to compare the gate field-induced channel conductivity per unit gate voltage, extracted by a product of mobility and the relative dielectric constant of the gate insulator.[4,6,8,23,50−61]

The trap density of states calculated by the S.S. value in PDPPFC24-TVT TFTs is ~5 × 10^{12} cm^{-2} eV^{-1}.[34]

To characterize charge transport properties, temperature-dependent field-effect mobility measurements were performed from 98 to 300 K. Figure 3A shows the plot of activation energies as a function of the channel carrier concentration. The activation energy decreases with an increasing carrier concentration. This decrease in activation energy fits the multiple trap and thermal release (MTR) or Monroe-type model of charge transport models.[35−38] The magnitude of the lowest activation energy (~40 meV) is relatively small in comparison to measurements made with other DPP-based semiconductors.[35,39−49] Activation energies of various high-mobility polymers are summarized in Figure 3B. These results show that DPP-based polymers have some of the lowest activation energies for carrier densities, <10^{13} cm^{-2}.[34]

We have devised a FOM to compare organics and polymers that have been reported thus far. The basic idea here is to compare the gate field-induced channel conductivity per unit gate voltage. This can be expressed as a product of mobility and the relative dielectric constant of the gate insulator (because the induced charge density is the product of capacitance per unit area and the gate voltage and the capacitance per unit area is proportional to the relative dielectric constant of the gate insulator). This has been plotted in Figure 4 for several polymer TFTs reported in the literature.[4,6,8,23,50−61] The TFT data reported for polymer PDPPFC24-TVT used in this study exhibits the highest FOM values, as compared to other studied materials. For practical applications, it is important to realize good performance at small channel lengths. Many materials exhibit significantly lower mobilities at small channel lengths. Thus, it makes sense to plot the FOM as a function of the channel length, which is shown in Figure 4. It can be observed that there are very few reports on high mobility organic/polymer TFTs with channel lengths less than 10 μm and most of the reported high-mobility TFTs do not have patterned gates, which are essential for any practical application. To calculate the FOM for multilayer gate dielectrics, we extracted an effective relative dielectric constant for the combination from the capacitance data and the combined physical thickness of all of the dielectrics.

A key aspect of our study is mainly attributed to the appropriate device geometry fabricated via rationally selected bilayer high-κ and low-κ dielectrics and novel donor−acceptor-based active organic semiconducting material. As per our knowledge, the obtained mobility value and FOM are both the one of the best values reported thus far using such a small channel length TFT device. Although some aspects of these

design features have been previously reported by various groups,[54,62,63] the combination of these design features in a single device has never been reported, and this is the key to the good performance. Firstly, we employed recessed gates that result in a much lower leakage current and improve better material organization of the gate insulator because sharp surface relief is avoided. The recessed-gate architecture also allows for lowering the gate insulator thickness without degrading the gate leakage current and on/off ratio. The thin second insulator is also very important for lowering the gate leakage current significantly and also provides a low-κ interface to the polymer semiconductor, which improves the polymer mobility, as pointed out above. The source drain contacts are defined by lithography but can also be fabricated by imprinting or laser ablation. We employ a single surface treatment of the contacts, with PFBT, to improve carrier injection into the polymer semiconductor. This is essential for channel lengths below 10 μm. The exact polymer semiconductor, PDPPFC24-TVT, has not been reported before, but the analogous structure with a shorter C_{20} branched alkyl chain was reported by our group earlier.[49] In recent years, there have been several reports of donor−acceptor materials, particularly those based on the diketopyrrolopyrrole core substituted with thiophene, but there are no reports on furan-substituted diketopyrrolopyrrole (DPPF) polymer with such an excellent mobility. Furan is one of the most promising heterocyclic blocks that has not been studied in detail before as thiophene and considered to be one of the important conjugated building blocks for making novel materials. Furan as an individual moiety is a highly unstable compound, but after combining it with DPP, it provides higher stability to the conjugated building blocks. The polymer semiconductor PDPPFC24-TVT reported in this work exhibits high molecular weight with excellent solution processability in many organic solvents because of longer branched alkyl chains. The highest occupied molecular orbital (HOMO) calculated by photoelectron spectroscopy in air (PESA) is 5.20 eV, which can be suitable for making air-stable organic electronic devices.

CONCLUSION

This report represents a major step forward, where the promise of organic semiconductors has been realized in a practical device geometry that can be advantageously used by many groups working in this field. The new semiconductor PDPPFC24-TVT is a very promising printable material for large-area, thin-film electronics and display applications. The device geometry used in this work is unique with a patterned, recessed gate and a small channel length of 4 μm, with an operating voltage below 10 V. The mobility is >4 $cm^2\ V^{-1}\ s^{-1}$, with an on/off current ratio of $\sim 10^7$, and the results reported in this report were measured in air. We also propose a FOM method that permits a meaningful comparison of reported TFTs.

ASSOCIATED CONTENT

Supporting Information

Characterization of materials and devices as well as details on synthesis and fabrication processes. This material is available free of charge via the Internet at http://pubs.acs.org.

AUTHOR INFORMATION

Corresponding Authors

*E-mail: sonarp@imre.a-star.edu.sg.

*E-mail: ananth.dodabalapur@engr.utexas.edu.

Notes

The authors declare no competing financial interest.

ACKNOWLEDGMENTS

The work on device fabrication, its characterization, and TFT transport studies was performed at The University of Texas at Austin and supported by the National Science Foundation (NSF) Nanomanufacturing Systems for Mobile Computing and Mobile Energy Technologies (NASCENT) Engineering Research Center (ERC). The chemical synthesis work was carried out at IMRE, Singapore, which was supported by A*STAR and the Visiting Investigator Program (VIP), for financial support. We are also thankful to the National Science Foundation, ECCS Division, for support.

REFERENCES

(1) Dodabalapur, A. *Mater. Today* **2006**, *9*, 24−30.
(2) Sirringhaus, H.; Tessler, N.; Friend, R. H. *Science* **1998**, *280*, 1741−1744.
(3) Crone, B.; Dodabalapur, A.; Lin, Y.-Y.; Filas, R. W.; Bao, Z.; LaDuca, A.; Sarpeshkar, R.; Katz, H. E.; Li, W. *Nature* **2000**, *403*, 521−523.
(4) Yan, H.; Chen, Z.; Zheng, Y.; Newman, C.; Quinn, J. R.; Dötz, F.; Kastler, M.; Facchetti, A. *Nature* **2009**, *457*, 679−686.
(5) McCulloch, I.; Heeney, M.; Bailey, C.; Genevicius, K.; MacDonald, I.; Shkunov, M.; Sparrowe, D.; Tierney, S.; Wagner, R.; Zhang, W.; Chabinyc, M. L.; Kline, R. J.; McGehee, M. D.; Toney, M. F. *Nat. Mater.* **2006**, *5*, 328−333.
(6) Ha, T.-J.; Sonar, P.; Dodabalapur, A. *Appl. Phys. Lett.* **2011**, *98*, 253305.
(7) Guo, X.; Silva, S. R. P. *Science* **2008**, *320*, 618−619.
(8) Li, J.; Zhao, Y.; Tan, H. S.; Guo, Y.; Di, C.-A.; Yu, G.; Liu, Y.; Lin, M.; Lim, S. H.; Zhou, Y.; Su, H.; Ong, B. S. *Sci. Rep.* **2012**, *2*, 1−9.
(9) Chen, H.; Guo, Y.; Yu, G.; Zhao, Y.; Zhang, J.; Gao, D.; Liu, H.; Liu, Y. *Adv. Mater.* **2012**, *24*, 4618−4622.
(10) Reese, C.; Bao, Z. *Mater. Today* **2007**, *10*, 20−27.
(11) Nielsen, C. B.; Turbiez, M.; McCulloch, I. *Adv. Mater.* **2013**, *25*, 1859−1880.
(12) Biniek, L.; Schroeder, B. C.; Nielsen, C. B.; McCulloch, I. *J. Mater. Chem.* **2012**, *22*, 14803−14813.
(13) Li, Y.; Sonar, P.; Murphy, L.; Hong, W. *Energy Environ. Sci.* **2013**, *6*, 1684−1710.
(14) Yuen, J. D.; Wudl, F. *Energy Environ. Sci.* **2013**, *6*, 392−406.
(15) Kang, I.; Yun, H. J.; Chung, D. S.; Kwon, S. K.; Kim, Y. H. *J. Am. Chem. Soc.* **2013**, *135*, 14896−14899.
(16) Gelinck, G. H.; Huitema, H. E. A.; Veenendaal, E. V.; Cantatore, E.; Schrijnemakers, L.; Putten, J. B. P. H.; Geuns, T. C. T.; Beenhakkers, M.; Giesbers, J. B.; Huisman, B.-H.; Meijer, E. J.; Benito, E. M.; Touwslager, F. J.; Marsman, A. W.; Rens, B. J. E.; Leeuw, M. *Nat. Mater.* **2004**, *3*, 106−110.
(17) Bao, Z.; Dodabalapur, A.; Lovinger, A. J. *Appl. Phys. Lett.* **1996**, *69*, 4108.
(18) Dimitrakopoulos, C. D.; Kymissis, I.; Purushothaman, S.; Neumayer, D. A.; Duncombe, P. R.; Laibowitz, R. B. *Adv. Mater.* **1999**, *11*, 1372−1375.
(19) Horowitz, G. *Adv. Mater.* **1998**, *10*, 365−377.
(20) Bao, Z. *Adv. Mater.* **2000**, *12*, 227−230.
(21) Facchetti, A.; Yoon, M.-H.; Marks, T. J. *Adv. Mater.* **2005**, *17*, 1705−1725.
(22) Sirringhaus, H.; Kawase, T.; Friend, R. H.; Shimoda, T.; Inbasekaran, M.; Wu, W.; Woo, E. P. *Science* **2000**, *290*, 2123−2126.
(23) Kanimozhi, C.; Yaacobi-Gross, N.; Chou, K. W.; Amassian, A.; Anthopoulos, T. D.; Patil, S. *J. Am. Chem. Soc.* **2012**, *134*, 16532−16535.
(24) Ong, B. S.; Wu, Y.; Liu, P.; Gardner, S. *J. Am. Chem. Soc.* **2004**, *126*, 3378−3379.

(25) Sundar, V. C.; Zaumseil, J.; Podzorov, V.; Menard, E.; Willett, R. L.; Someya, T.; Gershenson, M. E.; Rogers, J. A. *Science* **2004**, *303*, 1644−1646.
(26) Sonar, P.; Singh, S. P.; Li, Y.; Soh, M. S.; Dodabalapur, A. *Adv. Mater.* **2010**, *22*, 5409−5413.
(27) Sekitani, T.; Zschieschang, U.; Klauk, H.; Someya, T. *Nat. Mater.* **2010**, *9*, 1015−1022.
(28) Menard, E.; Podzorov, V.; Hur, S.-H.; Gaur, A.; Gershenson, M. E.; Rogers, J. A. *Adv. Mater.* **2004**, *16*, 2097−2101.
(29) Hulea, I. N.; Fratini, S.; Xie, H.; Mulder, C. L.; Iossad, N. N.; Rastelli, G.; Ciuchi, S.; Morpurgo, A. F. *Nat. Mater.* **2006**, *5*, 982−986.
(30) Duarte, D.; Dodabalapur, A. *J. Appl. Phys.* **2012**, *111*, 044509.
(31) Veres, J.; Ogier, S. D.; Leeming, S. W.; Cupertino, D. C.; MohialdinKhaffaf, S. *Adv. Mater.* **2003**, *13*, 199−204.
(32) Mathijssen, S. G. J.; Smits, E. C. P.; Hal, P. A.; Wondergem, H. J.; Ponomarenko, S. A.; Moser, A.; Resel, R.; Bobbert, P. A.; Kemerink, M.; Janssen, R. A. J.; Leeuw, D. M. *Nat. Nanotechnol.* **2009**, *4*, 674−680.
(33) Ha, T.-J.; Sparrowe, D.; Dodabalapur, A. *Org. Electron.* **2011**, *12*, 1846−1851.
(34) Rolland, A.; Richard, J.; Kleider, J. P.; Mencaraglia, D. *J. Electrochem. Soc.* **1993**, *140*, 3679−3683.
(35) Salleo, A.; Chen, T. W.; Völkel, A. R.; Wu, Y.; Liu, P.; Ong, B. S.; Street, R. A. *Phys. Rev. B: Condens. Matter Mater. Phys.* **2004**, *70*, 115311.
(36) Dimitrakopoulos, C. D.; Malenfant, P. R. L. *Adv. Mater.* **2002**, *14*, 99−117.
(37) Le Comber, P. G.; Spear, W. E. *Phys. Rev. Lett.* **1970**, *25*, 509.
(38) Monroe, D. *Phys. Rev. Lett.* **1985**, *54*, 146.
(39) Chang, J.-F.; Sirringhaus, H.; Giles, M.; Heeney, M.; McCulloch, I. *Phys. Rev. B: Condens. Matter Mater. Phys.* **2007**, *76*, 205204.
(40) Merlo, J. A.; Frisbie, C. *J. Polym. Sci., Part B: Polym. Phys.* **2003**, *41*, 2674−2680.
(41) Sirringhaus, H.; Brown, P. J.; Friend, R. H.; Nielsen, M. M.; Bechgaard, K.; Langeveld-Voss, B. M. W.; Spiering, A. J. H.; Ganssen, R. A. J.; Meijer, E. W.; Herwig, P.; de Leeuw, D. M. *Nature* **1999**, *401*, 685−688.
(42) Guo, J.; Ohkita, H.; Yokoya, S.; Benten, H.; Ito, S. *J. Am. Chem. Soc.* **2010**, *132*, 9631−9637.
(43) Wang, C.; Jimison, L. H.; Goris, L.; McCulloch, I.; Heeney, M.; Ziegler, A.; Salleo, A. *Adv. Mater.* **2012**, *22*, 697−701.
(44) Zhao, N.; Noh, Y.-Y.; Chang, J.-F.; Heeney, M.; McCulloch, I.; Sirringhaus, H. *Adv. Mat.* **2009**, *21*, 3759−3763.
(45) Kang, E. S. H.; Kim, E. *Org. Electron.* **2011**, *12*, 1649−1656.
(46) Matsui, H.; Kumaki, D.; Takahashi, E.; Takimiya, K.; Tokito, S.; Hasegawa, T. *Phys. Rev. B: Condens. Matter Mater. Phys.* **2012**, *85*, 035308.
(47) Kronemeijer, A. J.; Gili, E.; Shahid, M.; Rivnay, J.; Salleo, A.; Heeney, M.; Sirringhaus, H. *Adv. Mater.* **2012**, *24*, 1558−1565.
(48) Ha, T.-J.; Sonar, P.; Cobb, B.; Dodabalapur, A. *Org. Electron.* **2012**, *13*, 136−141.
(49) Sonar, P.; Zhuo, J.-M.; Zhao, L.-H.; Lim, K.-M.; Chen, J.; Rondinone, A. J.; Singh, S. P.; Chua, L.-L.; Ho, P. K.; Dodabalapur, A. *J. Mater. Chem.* **2012**, *22*, 17284.
(50) Ha, T.-J.; Sonar, P.; Dodabalapur, A. *Phys. Chem. Chem. Phys.* **2013**, *15*, 9735−9741.
(51) Jeong, Y.; Dodabalapur, A. *Appl. Phys. Lett.* **2007**, *91*, 193509.
(52) Klauk, H.; Halik, M.; Zschieschang, U.; Schmid, G.; Radlik, W.; Weber, W. *J. Appl. Phys.* **2002**, *92*, 5259.
(53) Reese, C.; Chung, W.-J.; Ling, M.-M.; Roberts, M.; Bao, Z. *Appl. Phys. Lett.* **2006**, *89*, 202108.
(54) Giri, G.; Verploegen, E.; Mannsfeld, S.; Atahan-Evrenk, S.; Kim, D.; Lee, S.; Becerril, H.; Aspuru-Guzik, A.; Toney, M.; Bao, Z. *Nature* **2011**, *480*, 504−508.
(55) Baeg, K.-J.; Khim, D.; Kim, J.; Kim, D.-Y.; Sung, S.-W.; Yang, B.-D.; Noh, Y.-Y. *IEEE Electron Device Lett.* **2013**, *34*, 126.
(56) Garnier, F.; Horowitz, G.; Peng, X.; Fichou, D. *Adv. Mater.* **1990**, *2*, 592−594.
(57) Zhong, H.; Smith, J.; Rossbauer, S.; White, A.; Anthopoulos, T.; Heeyney, M. *Adv. Mater.* **2012**, *24*, 3205−3211.
(58) Guo, X.; Ortiz, R.; Zheng, Y.; Kim, M.-G.; Zhang, S.; Hu, Y.; Lu, G.; Facchetti, A.; Marks, T. *J. Am. Chem. Soc.* **2011**, *133*, 13685−13697.
(59) Li, J.; Sun, Z.; Yan, F. *Adv. Mater.* **2012**, *24*, 88−93.
(60) Wei, P.; Menke, T.; Naab, B.; Leo, K.; Riede, M.; Bao, Z. *J. Am. Chem. Soc.* **2012**, *134*, 3999−4002.
(61) Chen, Z.; Lee, M.; Ashraf, R.; Gu, Y.; Albert-Seifried, S.; Nielsen, M.; Schroeder, B.; Anthopoulos, T.; Heeney, M.; McCulloch, I.; Sirringhaus, H. *Adv. Mater.* **2012**, *24*, 647−652.
(62) Podzorov, V.; Menard, E.; Borissov, A.; Kiryukhin, V.; Rogers, J. A.; Gershenson, M. E. *Phys. Rev. Lett.* **2004**, *93*, 086602.
(63) Ortiz, R. P.; Facchetti, A.; Marks, T. J. *Chem. Rev.* **2010**, *110*, 205−239.